ACS OMEGA

Open Access

This article is licensed under CC-BY-NC-ND 4.0

http://pubs.acs.org/journal/acsodf

Article

Physicochemical Characteristics and Their Variation of Coal Dust Originating from Underground Mining Sites

Yuzhu Zhou, Jianguo Liu,* Longzhe Jin, Gang Li, Gang Zhou, Minglei Lin, Shengnan Ou, Linquan Tong, Weijun Zhang, Xiaobing Wang, and Hong Gao

Cite This: *ACS Omega* 2025, 10, 5379−5394

Read Online

ACCESS | Metrics & More | Article Recommendations

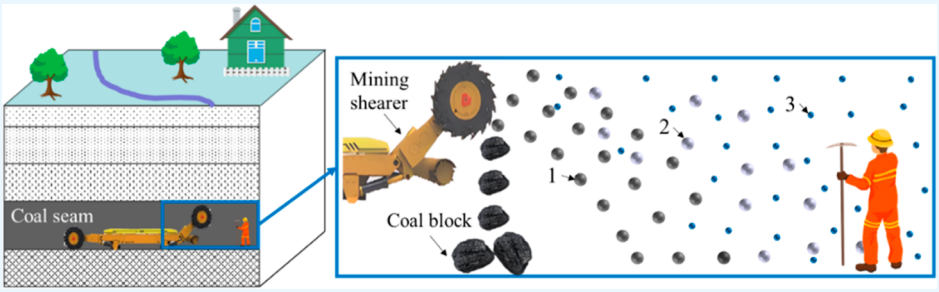

ABSTRACT: The physicochemical properties of coal dust significantly affect its toxicity and dust suppression efficiency. Currently, lab-crushed coal dust is commonly used for characterization instead of the original coal dust (OCD) sampled from underground mining sites. This practice leads to an inaccurate understanding of the underground coal dust properties. To address this issue, the study directly collected 18 OCD samples from various underground mining sites and characterized their physicochemical properties, and the variation of these physicochemical parameters of OCD with various coal rank were analyzed. The results show: OCD has a small particle size (average 26.49 μm), and around 21% of particles are under 10 μm. OCD has a well-developed pore structure, with an average total pore volume of 8.24×10^{-3} cm^3/g and an average specific surface area of 8.24 m^2/g. OCD samples have a high oxidation degree, and the average relative content of total oxygen-containing functional groups is 45.71%. Between the 32 measured physicochemical parameters of OCD, 10 moderately correlates with R_0 and 6 highly correlates with R_0. These parameters mainly involve wettability, pore structure, moisture content, and elemental composition. The findings present valuable insights into accurately assessing the toxicology and health risks of coal dust in underground mining sites and for selecting efficient dust control technologies in different coal mines.

1. INTRODUCTION

Coal dust is extremely harmful to human health and safety. First, coal dust has significant harmful effects on human health.[1−5] For example, inhaling coal dust can induce coal workers pneumoconiosis (CWP), a common occupational lung disease also known as black lungs or miners lungs.[6] Recently, an increasing trend in the number of CWP cases has been reported in China, with the annual number of CWP cases rising from 9173 in 2005 to 22701 in 2017; approximately 1900 people die of CWP each year.[7,8] Similar trends have emerged in other coal-producing countries, such as Australia and the USA.[9−11] Second, coal dust explosion is another serious hazard in underground that can result in heavy casualties.[12] In the Lijiagou coal mine (Shaanxi, China), on January 12th, 2019, a violent coal dust explosion caused 21 deaths;[13] between 1949 and 2007, there were reported 4613 casualties because of coal dust explosions in China.[14] Third, coal dust also has a significant pollution on environment,[1,3,15−17] and numerous studies have shown the changes in the contents of heavy metal elements and trace elements in the air and soil around coal mines.[3,18] Therefore, coal dust has significant harmful effects on human health, safe work, and environmental quality.

Extensive research has demonstrated that the physicochemical properties of coal dust play crucial roles in determining its toxicity to humans and the efficiency of dust control technologies.[19−22] Specifically, for the impact of the physicochemical properties of coal dust on its toxicity, Beer et al.[23] conducted a comprehensive review on the risk of developing interstitial lung diseases caused by coal dust. They discovered that the risk factors associated with CWP were

Received: July 21, 2024
Revised: January 19, 2025
Accepted: January 24, 2025
Published: February 3, 2025

© 2025 The Authors. Published by American Chemical Society

Figure 1. Sampling regional distribution map of the original coal dust.

mainly linked to coal characteristics, such as coal rank, quartz, and iron content. Furthermore, the particle size and shape of coal dust significantly influence human health as they can affect the deposition characteristics of dust within the lungs,[20,24,25] specifically, smaller coal dust particles are more detrimental to human health than larger particles.[26] In addition, the composition, functional groups, morphology, and other factors of coal dust also affect the occurrence of CWP.[20,21] For the impact of the physicochemical properties of coal dust on the efficiency of dust control technologies, Wang et al.[27] found a significant challenge lies in the strong hydrophobic characteristics exhibited by most coal dust. These properties hinder the rapid wetting of coal dust within the coal body when using coal seam water injection, consequently limiting its effectiveness in reducing dust. Furthermore, the wettability of coal dust is also a critical factor influencing the efficiency of spray dust suppression technology.[28−30] Factors, such as industrial components, surface functional groups, and elemental content of coal dust, can affect its wettability, thus influencing the dust removal efficiency of dust suppression technologies.[31−35] Also, the particle size of coal dust affects the inertial collision and interception actions between the dust and droplet particles, thus influencing the dust removal efficiency of the spray.[36,37] Furthermore, the surface pore structure of coal dust can influence its aerodynamic properties, potentially affecting its dispersion and settling characteristics.[19,33,38] In summary, the physicochemical characteristics of coal dust significantly impact human health and dust removal efficiency. Therefore, the characterization of the physicochemical properties of coal dust is of great significance.

Currently, lab-crushed dust is typically used to characterize the physicochemical properties of coal dust.[28,35,39−41] Lab-crushed dust is prepared by grinding coal fragments in the laboratory mostly through ball milling. Coal dust is generated through the collision force of a grinding medium, such as a steel shot or alumina balls.[42] In contrast to laboratory-crushed dust, the original coal dust (OCD) from underground mining sites is generated because of the breakage of coal rock under the cutting force of shearers.[43] The large particles in the original coal dust (OCD) would settle down under the force of gravity; only fine dust particles can float in the mine air, which could be inhaled by workers. However, there is no gravity-settling process when producing lab-crushed dust; therefore, large and fine dust particles are all combined in lab-crushed dust. Because of these differences, the physicochemical properties tested with lab-crushed dust may differ from the OCD collected directly from underground mining sites. As reported by Trechera et al.,[44] in the underground coal mining face, the maximum mass fraction of respirable dust (particle size $\leq$10 μm, i.e. PM10) reaches 65.6%, which is much greater than the respirable dust content in lab-crushed dust. Similar results were also reported by Kollipara et al.,[45] who found that close to the shearer, the maximum mass fraction of respirable dust reached 68%. In additionally, many studies show that the physical and chemical characteristics of coal dust have a direct impact on the dust removal efficiency of spray technology, chemical dust suppressants and wet dust collector.[19,21,28−31,33] However, the current misunderstanding of the physicochemical characteristics of underground coal dust greatly limits the optimization of the dust removal technologies. Therefore, using lab-crushed coal dust to characterize the physicochemical properties of OCD could mislead assessments of the toxicity of coal dust and misguide selection of dust control technologies in underground mining processes.

Herein, the present study aimed to investigate the physicochemical properties of OCD directly collected from underground mining sites. We successfully collected 18 coal dust samples from different underground mining faces in China and systematically characterized their physicochemical properties, including wettability, particle size, pore structure, maceral content, proximate components, surface elements, and chemical functional groups. Finally, the correlations between the physicochemical parameters of OCD and its coal rank (maximum vitrinite reflectance, R_0) were analyzed using the

https://doi.org/10.1021/acsomega.4c06729
ACS Omega 2025, 10, 5379−5394

Spearman and Pearson correlation coefficient. This study provided accurate values of physicochemical characteristics of coal dust with various coal ranks produced in underground mining sites. This can give insight into assessing the toxicity of coal dust and selecting efficient dust control technologies for underground mining processes.

2. MATERIAL AND METHODS

2.1. Sampling Method. OCD samples were collected from 18 underground mining sites across nine cities in China (Figure 1) using the gravimetric sampling method. Compared to the sampling method of filter membrane, the gravity sampling method can obtain more coal dust samples, which is convenient for the subsequent characterization of the physicochemical properties of coal dust. The method was described in our previous study;[38] specifically, a steel salver was hung from the roof of the return airway at 1.5 m height (the average breathing height of Chinese[46]) for 8 h and about 10 m from the working face when shearer was working. The collected OCD samples were screened through a 200 mesh (about 74 μm) to remove large particles that fell from the roof. Finally, the samples were packed into a sealed plastic pouch and immediately brought back to the lab for physicochemical properties tests.

Block coal from underground mining sites was also sampled according to GB/T 482-2008 to obtain the coal rank of the sampled coal dust. The maximum vitrinite reflectance (R_0) of block coal was measured according to GB/T 6948-2008, and the coal rank was obtained based on R_0 value following ISO 11760:2018. Table 1 presents the coal ranks of the studied coal samples. It could be observed that almost all coal ranks, from sub-bituminous to anthracite C, were included in the studied 18 coal samples.

Table 1. Maximum Vitrinite Reflectance (R_0) and Coal Ranks of the Studied Coal Samples

number	district	sample name	R_0/%	coal rank
1	Shenmu	SM-1	0.42	sub-bituminous
2	Shenmu	SM-2	0.49	sub-bituminous
3	Shenmu	SM-3	0.51	bituminous d
4	Yanbian	YB	0.53	bituminous d
5	Erdos	ED-1	0.54	bituminous d
6	Erdos	ED-2	0.54	bituminous d
7	Erdos	ED-3	0.59	bituminous d
8	Datong	DT-1	0.60	bituminous c
9	Datong	DT-2	0.61	bituminous c
10	Baiyin	BY-1	0.67	bituminous c
11	Datong	DT-3	0.70	bituminous c
12	Wuhai	WH-1	0.94	bituminous c
13	Wuhai	WH-2	1.00	bituminous c
14	Yongcheng	YC-1	1.32	bituminous b
15	Lvliang	LL	1.48	bituminous a
16	Changzhi	CZ-1	1.99	bituminous a
17	Changzhi	CZ-2	2.10	anthracite c
18	Yongcheng	YC-2	2.44	anthracite c

2.2. Characterization and Analyses. Figure 2 shows the physicochemical parameters and the corresponding measurement methods of the OCD samples. Briefly, seven physicochemical properties (particle size, elements, pore parameters, industrial components, wettability, vitrinite components, and surface carbon functional groups) of the OCD were determined using various methods and instruments. Reportedly, these properties have shown significant effects on dust control efficiency and toxicology.[19,20,23,47] The detailed characterization methods for these parameters are described in the following subsections.

2.2.1. Particle Size Test. The particle size of coal dust determines its inhalability by the human body and significantly affects its settling characteristics, wettability, and explosiveness.[20,21,48,49] The particle size distributions of the OCD samples were tested using a laser particle size analyzer (Winner 2000, China). To improve the dispersibility of coal dust in the solution, an alcohol solution with a mass concentration of 75% was used as the dispersing medium.[50] A typical particle size distribution of coal dust is shown in Figure 3. To quantitatively analyze the variation of particle size, the particle diameter corresponding to the cumulative percentages of 10, 50, and 90 (D10, D50, and D90, respectively) and the cumulative percentage of particles with a diameter less than 10 μm (P10) were selected as the characteristic parameters, as shown in Figure 3. Smaller values of D10, D50, and D90 and larger values of P10 indicated a smaller particle size distribution of the dust particles.

2.2.2. Determination of Pore Parameters. The pore parameters of coal dust significantly affect its wettability and aerodynamic characteristics, which in turn affect the efficiency of coal dust control.[19,39,48] In this study, a low-pressure N_2 gas adsorption (LP-N2GA) analysis method and various calculation models (Table 2) were used to test the micropore and mesopore parameters of coal dust.[51] According to GB/T 21650.3-2011, experiments were conducted at atmospheric pressure with liquid nitrogen (77 K, 101.3 kPa) using a 3H-2000PS2 instrument. Subsequently, based on various calculation models (Table 2), the specific surface area (SSA), pore size, and pore volume of the micropores and mesopores in the OCD samples were calculated. The testing methods and sample processing procedures are explained in detail in our previous study.[38]

2.2.3. Ultimate Analysis. The elements of coal dust significantly influence its wettability and toxicology.[35,56] Using a coal elemental analyzer (HCCH-3000), the relative contents of C, H, O, N, and S in the OCD samples were tested according to the standard GB/T 31391-2015. The O content was calculated using the differential subtraction method.[57]

2.2.4. Industrial Component Analysis. The industrial components of coal significantly influence the generation, dispersion, and control efficiencies of coal dust.[19] For example, as the moisture content increases, coal mining becomes less prone to dust generation.[38] According to ISO 11722:2013, the relative contents of the industrial components of the 18 OCD samples were tested using an automatic industrial analyzer (GF-A2000), where moisture, ash, and fixed carbon were measured on an air-dried basis, volatile matter was measured on a dry ash-free basis.

2.2.5. Wettability Test. In underground coal mines, water-based dust control methods such as spraying, wet scrubbers, and foam are widely used for coal dust control.[19] Therefore, the wettability of coal dust plays a crucial role in the dust control efficiency. The initial contact angle is a commonly used parameter for characterizing the wettability of coal dust.[50,57] The initial contact angle between coal dust and water was tested using a Theta Lite apparatus (made in Finland). The testing principle of the instrument is illustrated in Figure 4a.[58] Detailly, during the testing process, about 1 g of coal dust was

https://doi.org/10.1021/acsomega.4c06729
ACS Omega 2025, 10, 5379−5394

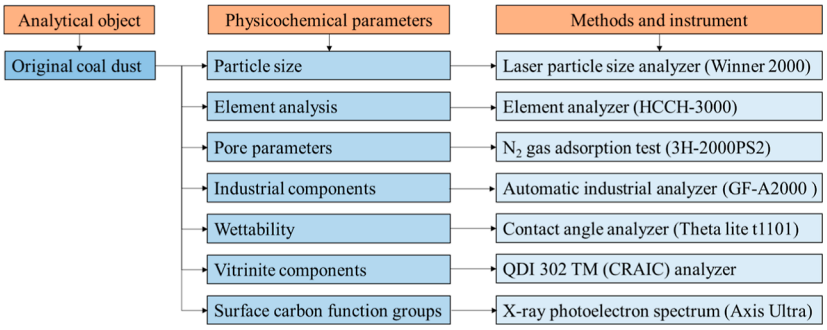

Figure 2. Physicochemical parameters and the corresponding measurement methods of the original coal dust.

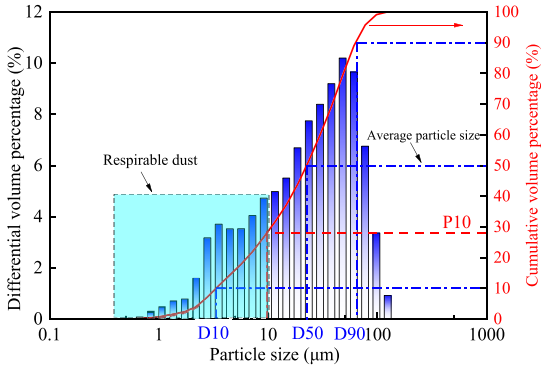

Figure 3. Characterization parameters of coal dust particle size.

Table 2. Calculation Models of the Pore Parameters of Coal Dust

pore characteristic	pore type	computation model	references
specific surface area (SSA)	micro- and mesopore	Brunauer–Emmett–Teller (BET)	Brunauer et al.[52]
pore size	micropore	Horváth–Kawazoe (HK)	Horváth and Kawazoe[53]
	mesopore	Barret–Joyner–Halenda (BJH)	Barrett et al.[54]
pore volume	micropore	density functional theory (DFT)	Seaton et al.[55]
	mesopore	Barret–Joyner–Halenda (BJH)	Barrett et al.[54]

compressed at 20 MPa in a mold with a diameter of 8 mm to form a coal dust cake. A water droplet was slowly dropped onto the coal dust cake, and a high-speed camera captured the moment of contact between the droplet and the coal dust. The OneAttension software was used to obtain the initial contact angle between the coal dust and the droplet (average of the left and right angles).

2.2.6. Maceral Composition Measurement. Coal is a mixture of complex organic and inorganic materials.[51] The four microscopic components of coal, namely, vitrinite, exinite, inertinite, and inorganic mineral groups, are important characterization parameters for the composition of coal. According to ISO 7404-5:2009, the relative mass percentages of the four maceral compositions were obtained using an automatic coal rock microscopy analysis instrument (Zeiss MY5000).

2.2.7. Determination of Surface Carbon Function Groups. Precisely identifying the specific components of coal dust using current detection techniques is difficult because it is a type of heterogeneous sedimentary rock.[59] Therefore, detecting the elements, macromolecular structures, and functional groups of coal dust is the main approach to investigate its chemical properties. Compared to Fourier transform infrared (FTIR) spectroscopy, X-ray photoelectron spectroscopy (XPS) can better reflect the surface features of the testing sample and hence assess the surface elemental content and functional groups as its detection depth is <10 nm for organic matter.[60] Therefore, XPS was conducted for the collected OCD samples on an Axis Ultra device with an Al Ka radiation source. During data analysis, the binding energies were calibrated at 284.8 eV for C 1s.[61] Then, the relative contents (RCs) of C, O, and Si were obtained by peak fitting method for the wide spectrum using XPS peak software. Equation 1[62] was used for calculations

$$N_i = \frac{\frac{S_i}{W_i}}{\sum_{i=1}^{n}\left(\frac{S_i}{W_i}\right)} \quad (1)$$

where N_i is the RC of element i; S_i and W_i are the peak areas on the wide spectrum and relative sensitivity factor of element i, respectively; and n is the number of elements.

The surface carbon functional groups of the OCD samples were identified and quantified using a multipeak fitting method for the C 1s narrow spectrum. As shown in Figure 5, peaks at binding energies of 284.6, 285.6, 286.6, and 289.1 eV correspond to the groups of aliphatic hydrocarbons (C–C/

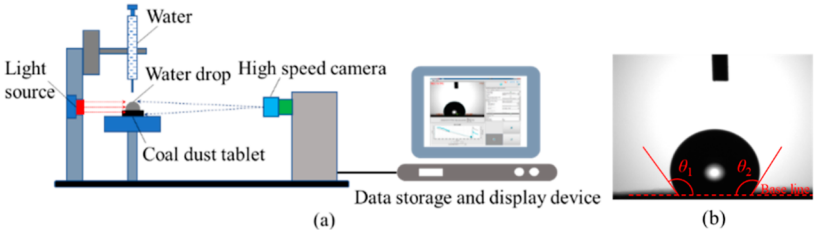

Figure 4. Schematic diagram of the initial contact angle testing instrument (a) and the contact angle between coal dust and water droplet (b).

https://doi.org/10.1021/acsomega.4c06729
ACS Omega 2025, 10, 5379–5394

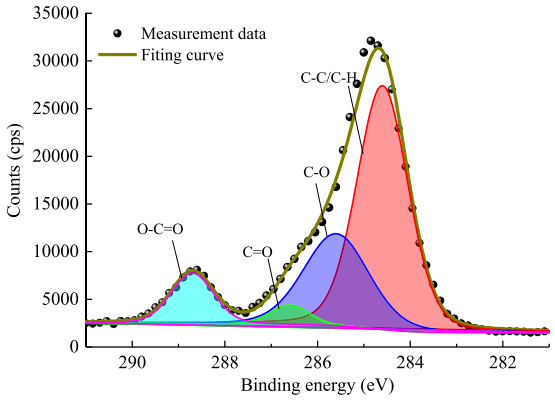

Figure 5. Schematic representation of peak fitting for the surface chemical functional groups of coal dust.

C−H), epoxy and alkoxy (C−O), carbonyl carbon (C═O), and carboxylate carbon (O−C═O), respectively.[63] The RC value of each carbon functional group was obtained by calculating the relative peak areas.

2.3. Correlation Methods. Spearman and Pearson correlation coefficient is commonly used to assess the correlation between two variables;[64−66] the formulas for calculating the coefficient of Spearman and Pearson are shown in eqs 2 and 3, respectively. The correlation coefficient between the physicochemical parameters of the OCD samples and its R_0 were calculated, and their relation intensity was estimated according to the values of ρ_1 and ρ_2, as shown in Table 3.

$$\rho_1 = \frac{\sum_{i=1}^{N}(R_i - \overline{R})(S_i - \overline{S})}{[\sum_{i=1}^{N}(R_i - \overline{R})^2 \sum_{i=1}^{N}(S_i - \overline{S})^2]^{1/2}} \quad (2)$$

Table 3. Relation Intensity According to Spearman and Pearson Correlation Coefficient Value

number	absolute value of correlation coefficient	relation intensity
1	0.0−0.2	no relation
2	0.2−0.4	weak relation
3	0.4−0.6	medium relation
4	0.6−0.8	strong relation
5	0.8−1.0	very strong relation

where ρ_1 is the Spearman correlation coefficient, R_i is the grade of ith value of parameter R, $\overline{R}$ is the average value of parameter R, S_i is the grade of ith value of parameter S, and $\overline{S}$ is the average value of parameter S.

$$\rho_2 = \frac{\sum_{i=1}^{N}(x_i - \overline{x})(y_i - \overline{y})}{[\sum_{i=1}^{N}(x_i - \overline{x})^2 \sum_{i=1}^{N}(y_i - \overline{y})^2]^{1/2}} \quad (3)$$

where ρ_2 is the Pearson correlation coefficient, x_i is the ith value of parameter x, $\overline{x}$ is the average value of parameter x, y_i is the ith value of parameter y, and $\overline{y}$ is the average value of parameter y.

ρ_1 Represents the consistency of one variable with the other, and ρ_2 represents the linear consistency of one variable with the other.

3. RESULTS

3.1. Particle Size Distribution of OCD. The variations of particle size of OCD with R_0 are shown in Figure 6. The D10 of the coal dust exhibited fluctuations as R_0 increased with an average of 5.64 μm (Figure 6a). The variations in D50 and in D90 were like that in D10 with an average of 26.49 and 65.83 μm, respectively (Figure 6b,c). The maximum, average, and minimum values of respirable dust fraction (P10) were 42.0%, 21.00%, and 9.73%, respectively (Figure 6d). Trechera et al.[67] measured the particle size of underground OCD in Central Eastern Europe and found that the proportion of coal dust with particle size <10 μm was about 17%, consistent with the results obtained in this study. However, Cheng et al.[68] found that 87.2% of pulverized coal has a particle size ranging between 177−250 μm. Furthermore, to characterize the physicochemical properties of coal dust, many studies[35,65,69,70] have utilized crushed coal sieved through a 200-mesh screen as a research sample. In comparison to the particle size of lab-crushed coal particles, that of coal dust generated in underground mines is significantly smaller with particle sizes well below 74 μm. Therefore, lab-crushed coal particles are not a substitute for OCD to characterize their physical and chemical parameters.

3.2. Pore Parameters of the OCD. *3.2.1. Pore Size.* With the increase of R_0, the size of the micropore and mesopore and the average pore size of OCD samples follows cubic function; that is, the pore size first increases around R_0 < 1%, decreases around 1% < R_0 < 2%, and then increases again when R_0 > 2% (Figure 7). The average micropore, mesopore, and pore sizes are 1.15, 8.99, and 11.82 nm, respectively, which were much smaller than the pore sizes of coal dust milled in laboratories.[51,71] The results indicated that the pore structure of the OCD samples was much more developed than that of coal dust prepared using a ball mill in the laboratory.

3.2.2. Pore Volume. The micropore, mesopore, and total pore volumes of the OCD samples decreased exponentially with increasing R_0 (Figure 8). Smaller the coal rank, larger the pore volume in the coal dust, resulting in a more developed pore structure. The average values of the micropore volume, mesopore volume, and total pore volume were 3.46, 19.39, and 8.24×10^{-3} cm^3/g, respectively. These values were higher than those reported earlier,[51] further demonstrating that the pore structure of the OCD samples is more developed than that of the lab-crushed coal dust.

3.2.3. Specific Surface Area. The SSA of the OCD samples are shown in Figure 8d. Similar with the variation of the pore volume, the SSA of OCD decreased exponentially with an increase in R_0 with an average of 8.24 m^2/g. This result indicates that the pore structure becomes more developed as the pore volume of the coal dust increases and the SSA increases. Yang et al.[40] reported that the average SSA of four lab-crushed coal dust samples ranged from 1.433 to 3.093 m^2/g. Therefore, it can be concluded that the surface pore structure of OCD is much more developed than that of the lab-crushed coal dust.

3.3. Ultimate Variation of OCD. The relative C, O, N, H, and S contents of the OCD samples are shown in Figure 9. The C content in the OCD exhibited a weak linear increase (R^2 = 0.17) with an increase in R_0, ranging from 36.11% to 81.43% with an average of 62.03% (Figure 9a). In contrast, the O content in the OCD exhibits a weak linear decrease (R^2 = 0.14) with an increase in R_0 ranging from 60.92% to 12.03%,

https://doi.org/10.1021/acsomega.4c06729
ACS Omega 2025, 10, 5379−5394

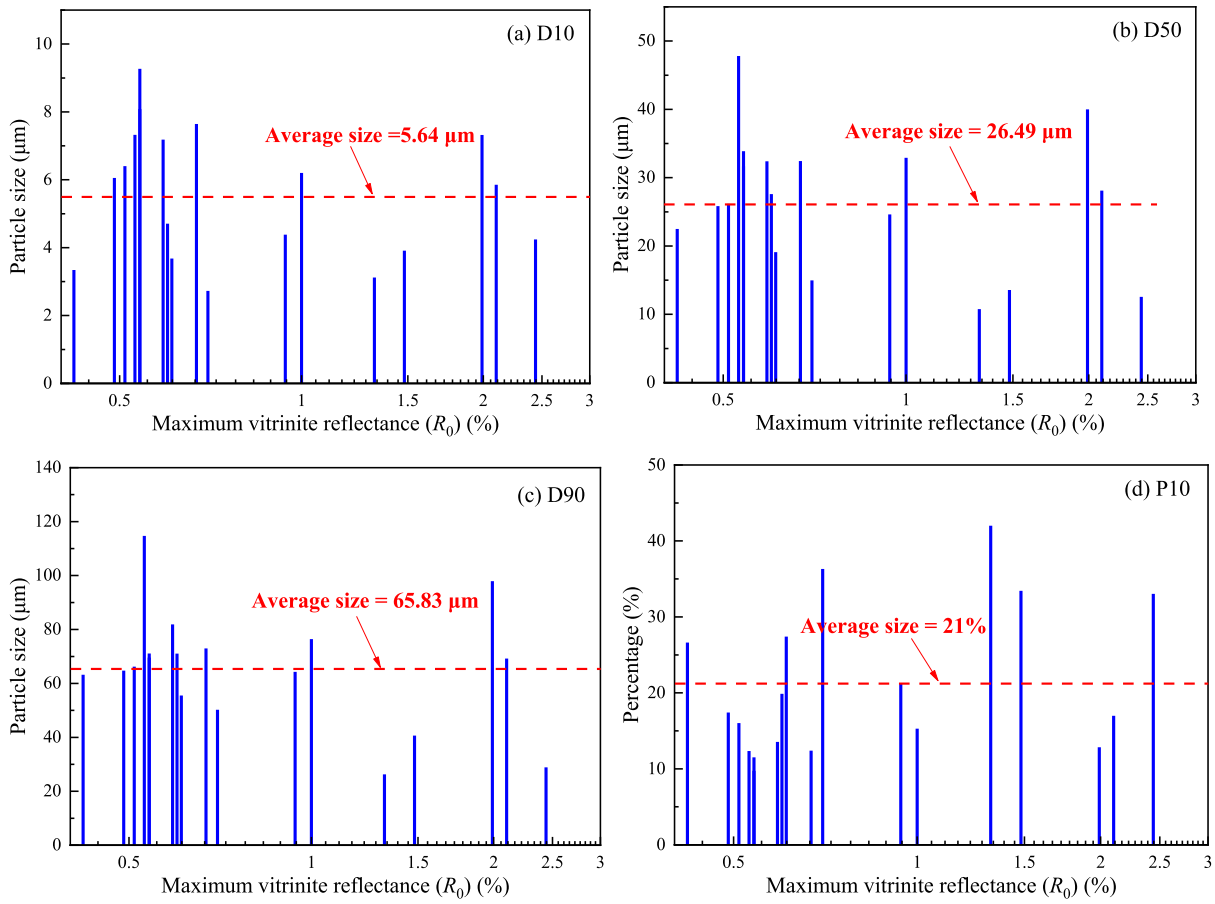

Figure 6. Variation of the particle size of OCD samples with R_0: D10 (a), D50 (b), D90 (c), and P10 (d).

with an average of 32.35% (Figure 9b). This is because as the coal rank increases, the degree of coal oxidation decreases, leading to an increase in the relative content of C and a decrease in the relative content of O in coal dust.

Similar to the variation pattern of C, the relative content of N in the OCD samples demonstrated an approximately linear upward trend (with a coefficient of determination $R^2 = 0.41$) as R_0 increased, as illustrated in Figure 9c. Nevertheless, it should be noted that the content of N was comparatively low, varying from 0.45% to 1.25% and averaging at 0.85%. Additionally, the average contents of H and S were relatively modest, standing at 3.68% and 1.09% respectively, as shown in Figure 9d,e. Hence, it can be concluded that the main differences in the RCs of elements in OCD samples are primarily in C and O. Using energy dispersive spectrometry, Zazouli et al.[56] found that O was more prevalent than C in the respirable coal dust generated in underground coal mines, indicating a higher oxidation degree on the surface of the respirable coal dust, which is consistent with the results of this study. However, Zhou et al.[60] analyzed six lab-crushed coal dust samples and found that the C content ranged from 70% to 90%, while the O content was below 15%. He et al.[72] studied 13 coal samples and found that the C content was >70%, whereas the O content was <10%. Therefore, it can be concluded that the oxidation degree of OCD was much higher than that of lab-crushed coal dust.

3.4. Industrial Component Variation of OCD. The industrial composition of coal dust significantly affects its wetting properties.[38] The moisture content of the OCD decreased exponentially with increasing R_0 (Figure 10a). This variation was like that of the pore volume and SSA (Figure 8). The moisture in coal dust is primarily adsorbed into its pore structure; therefore, the more developed the pore structure, the higher the moisture content.[38] The volatile content of the OCD decreased exponentially with increasing R_0 ($R^2 = 0.81$) (Figure 10b), indicating that higher-ranked coal dust had lower volatile content. This result is consistent with the study published previously,[73] which indicates that the volatile matter content of coal did not change significantly after it was crushed into coal dust. In addition, the ash content of the OCD fluctuated irregularly between 51.09% and 5.50% with an average of 22.80% (Figure 10c). In contrast, the fixed C in the coal dust increased logarithmically with increasing R_0 with an R^2 value of 0.45 (Figure 10d).

3.5. Contact Angle of OCD. Contact angle is a commonly used parameter to characterize the wettability of coal dust.[50,57] As R_0 increases, the wettability of the OCD increases logarithmically ($R^2 = 0.40$) (Figure 11). Specifically, when R_0 is between 0.4%−0.75%, most contact angles are less than 80°, indicating that coal dust is hydrophilic. When R_0 exceeded 0.75%, the contact angle remained relatively unchanged at approximately 120°, except for in Sample 15, indicating the coal dust was strongly hydrophobic. The contact angle of Sample 15 is 78°, which may be caused by the admixture of soot powder during the sampling process. Based on these results, it can be concluded that the coal rank significantly influences the wettability of coal dust.

3.6. Vitrinite Component of OCD. The variation in the maceral components of the OCD with R_0 is shown in Figure 12. As R_0 increased, the exinite content in the OCD showed a

https://doi.org/10.1021/acsomega.4c06729
ACS Omega 2025, 10, 5379−5394

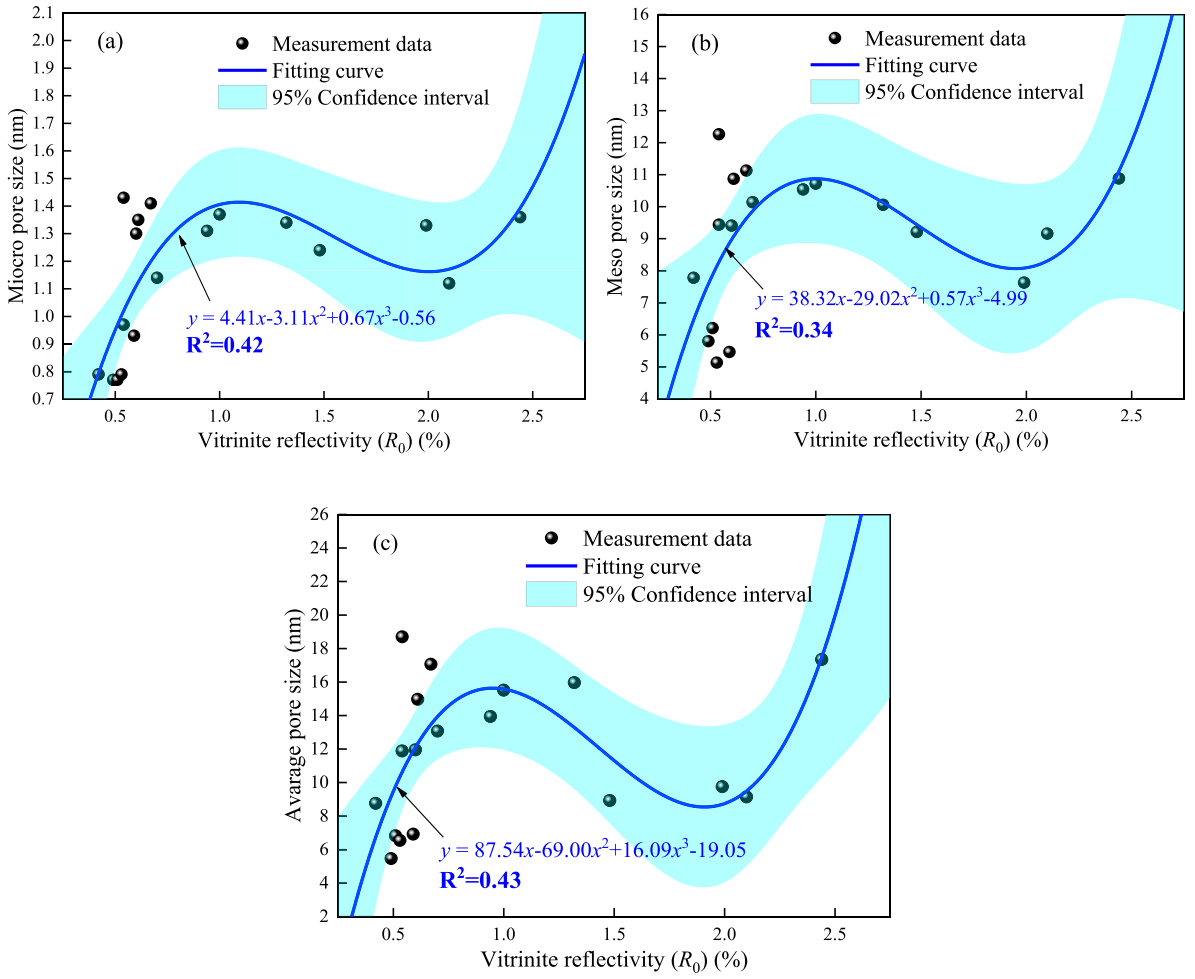

Figure 7. Variation of the pore size of OCD samples with R_0: micropore size (a), mesopore size (b), and average pore size (c).

weak logarithmic decreasing trend (R^2 = 0.36), with an average value of 10.36%. The other three components (vitrinite, inertinite, and inorganic minerals) exhibited irregular changes with increasing R_0 with average values of 71.03%, 0.74%, and 18.17%, respectively. This indicates that vitrinite was the predominant maceral component in the OCD, and coal rank did not significantly affect the maceral composition of the OCD.

3.7. Surface Carbon Function Groups of OCD. The elements of O, C, and Si in the OCD were tested using X-ray photoelectron spectroscopy (XPS), as shown in Figure 13.

Based on the maximum peak of each element in Figure 13, the RCs of C, O, and Si were calculated, and the results were shown in Figure 14. Except for in Sample 4, the average RCs of C, O, and Si were 67.22%, 27.45%, and 5.33%, respectively. Compared with rock dust, there is relatively little Si content in the OCD.

The distribution of the surface carbon functional groups on coal dust significantly affects its wettability.[60] As show in Figure 15, with increasing R_0, the RCs of the four carbon functional groups on the OCD surface exhibited irregular changes. The content of hydrophobic groups C−C and C−H was the highest, averaging 54.29%, and the average content of C−O groups was 32%. The contents of C═O and O−C═O groups averaged 9.86% and 3.85%, respectively. Compared with the results reported in previous studies,[60,74] the contents of C−C and C−H on the OCD surface were lower than those of lab-crushed coal dust, indicating that OCD has a higher degree of surface oxidation. Additionally, previous studies[72,75] have shown that the C and O functional groups on the coal surface exhibit regular changes with increasing R_0, which much differs with the results in this study.

3.8. Correlation Analysis of the Physicochemical Parameters of OCD and R_0. Herein, 32 physicochemical parameters of OCD were obtained through various tests. These parameters are listed in Table 4. The Spearman and Pearson correlation coefficients between the 32 physicochemical parameters of OCD and R_0 were calculated, and the results are shown in Figure 16.

Among 32 physicochemical parameters of OCD, 10 parameters had a moderate correlation (absolute value of ρ between 0.4 and 0.6) with R_0. Among these 10 parameters, four parameters positively correlated (i.e., contact angle, micropore size, average pore size, and relative content of C) and six negatively correlated with R_0 (i.e., specific surface area, micropore volume, relative content of O, relative content of O−C═O group, and inertinite content). Furthermore, six parameters correlate highly (absolute value of ρ between 0.6 and 0.8) with R_0. Among these six parameters, two positively correlated (fixed carbon content and relative content of N) and four negatively correlated (mesopore volume, total pore volume, moisture content, and volatile content) with R_0. The coal rank significantly influenced 14 physicochemical parameters, especially wettability, pore structure, moisture content,

https://doi.org/10.1021/acsomega.4c06729
ACS Omega 2025, 10, 5379−5394

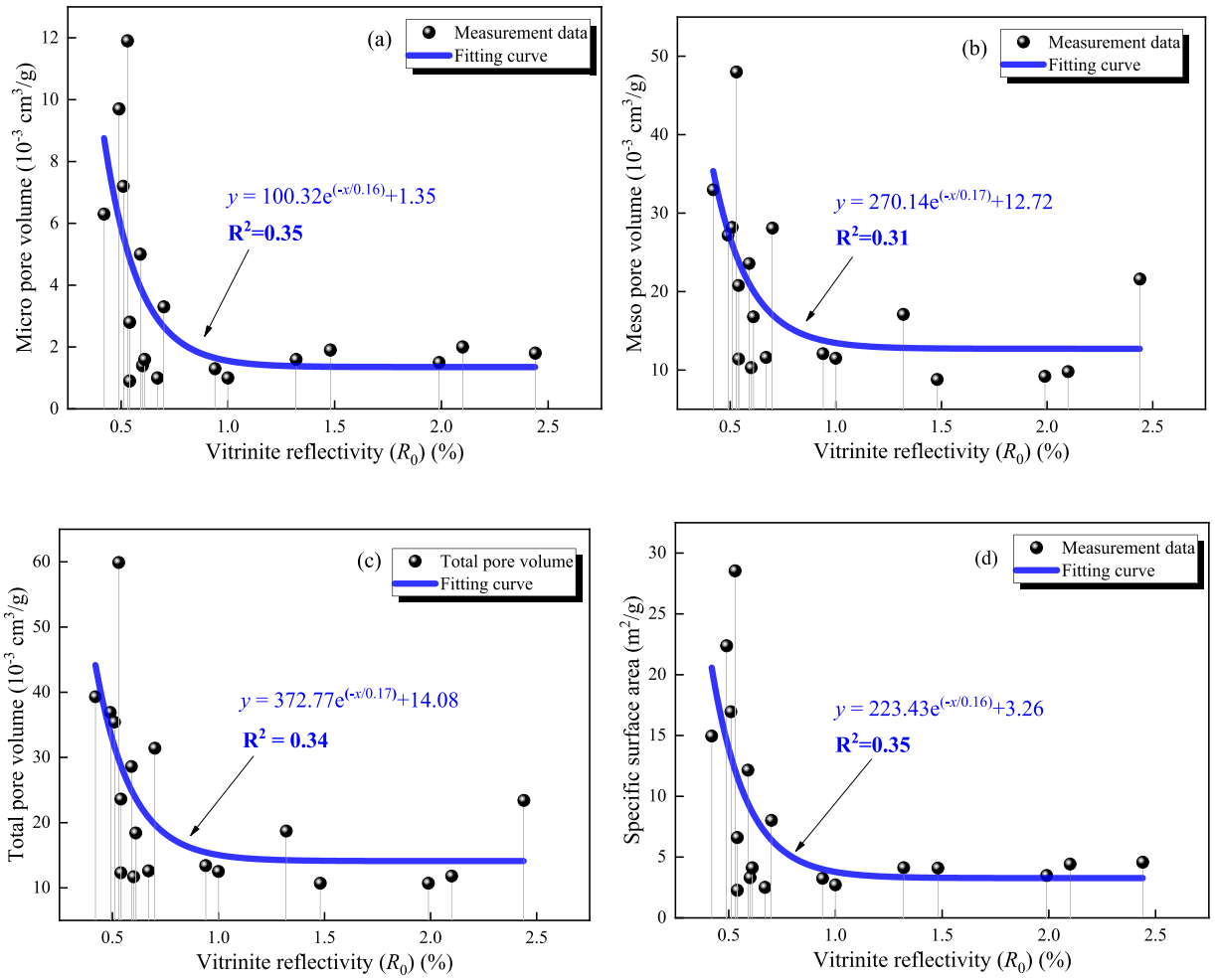

Figure 8. Variation of the pore volume and specific surface area (SSA) of OCD samples with R_0: micropore volume (a), mesopore volume (b), total pore volume (c), and SSA (d).

and elemental content, of OCD. That is, as the coal rank increases, the wettability of coal dust becomes worse and the porosity development degree decreases. The reduction in wettability decreases the efficiency of wetting dust suppression technology. Therefore, for the coal dust with large R_0, wetting agents should be considered for addition to reduce the surface tension of the solution and improve the wettability of coal dust to enhance the dust suppression efficiency, when applying the wetting dust suppression technology such as spray. The more developed the pores of coal dust are, the larger its specific surface area becomes. Consequently, the diffusion time and distance in the air will be extended, and the likelihood of being inhaled by humans will increase correspondingly. In contrast, the coal dust with low R_0 features a well-developed pore structure along with favorable wettability. Thus, wetting dust suppression technology can be widely adopted in underground mines. Besides, on the one hand, the positive and negative opposites of the Spearman and Pearson correlation coefficients for the parameters numbered 21 (element S), 23 (function group C−O), 27 (element O) and 32 (inorganic minerals), indicate that these parameters are not linearly varied with coal ranks; on the other hand, the values of the Spearman and Pearson correlation coefficients for the parameters numbered 14 (volatile), 16 (fixed carbon) and 20 (element N) are very close and all greater than 0.6, indicating that these parameters are not only strongly correlated with coal ranks but also linearly correlated.

4. DISCUSSION

The results of this study indicate that the original coal dust (OCD) generated from underground mining sites exhibits typical characteristics of small particle size, well-developed porosity, and a high degree of oxidation. Specifically, the average particle size of the 18 OCD samples is 26.49 μm, and approximately 21% of the dust particles being smaller than 10 μm. The average pore volume and specific surface area of the 18 OCD samples are 8.24×10^{-3} cm^3/g and 8.24 m^2/g, respectively. The average oxygen functional group content in the OCD samples is 45.71%. Furthermore, the physicochemical properties of coal dust show significant correlations with coal rank (R_0); among measured 32 physicochemical parameters, wettability, pore structure parameters, moisture content, and elemental composition of the OCD exhibit strong correlations with R_0.

4.1. Particle Size of the OCD. The particle size of the OCD samples is significantly smaller than the lab-crushed coal dust particle size reported in the literature.[68] As shown in Figure 17a, coal chunks and large- and small-particle were produced after a shearer crushed the coal body. Among them, coal chunks and large-particle coal dust settle quickly owing to gravity, whereas small-particle dust can diffuse in the roadway

https://doi.org/10.1021/acsomega.4c06729
ACS Omega 2025, 10, 5379−5394

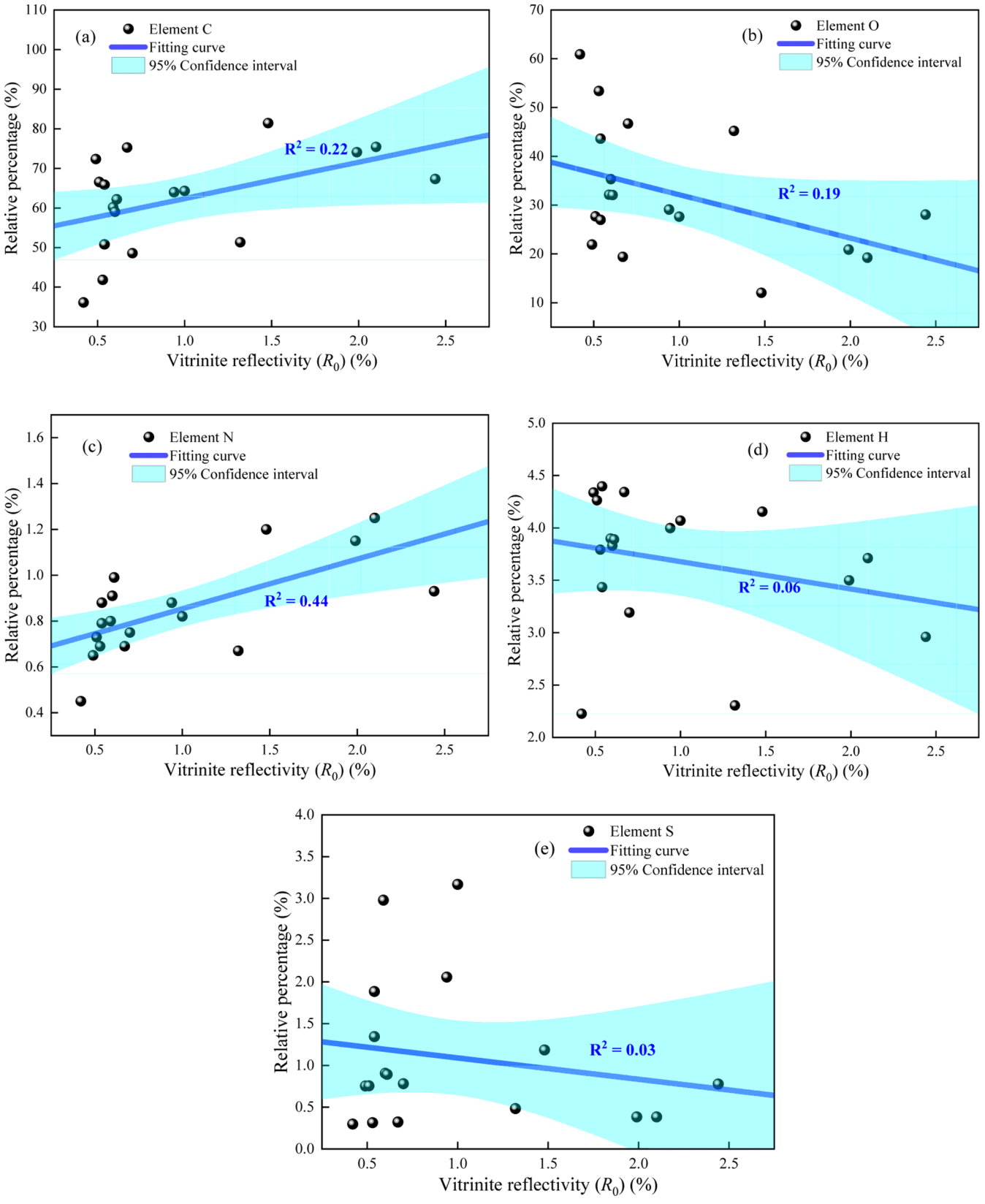

Figure 9. Variation of the element contents in OCD samples with R_0: C (a), O (b), N (c), H (d), and S (e).

under the influence of airflow. This significantly increases the probability of OCD being inhaled by humans, thereby augmenting the harm of coal dust to the human body.[38] However, large- and small-particle dust is mixed in lab-crushed coal dust. Therefore, it is inaccurate to use lab-crushed coal dust to characterized the physicochemical properties of the original coal dust from underground mining sites. The result provides an accurate basis for the performance improvement of

https://doi.org/10.1021/acsomega.4c06729
ACS Omega 2025, 10, 5379−5394

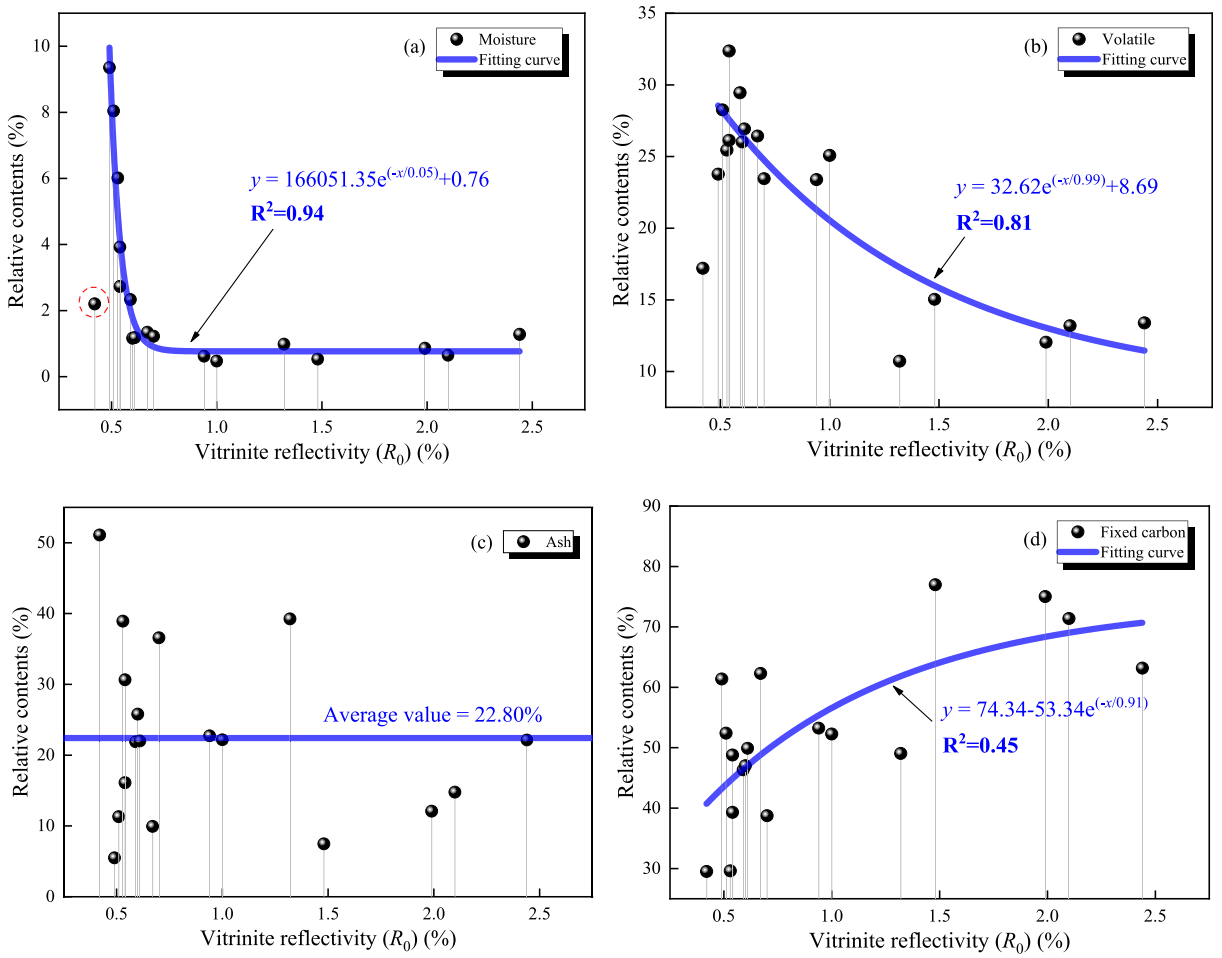

Figure 10. Variation of the industrial component of OCD samples with R_0: moisture (a), volatile (b), ash (c), and fixed carbon (d).

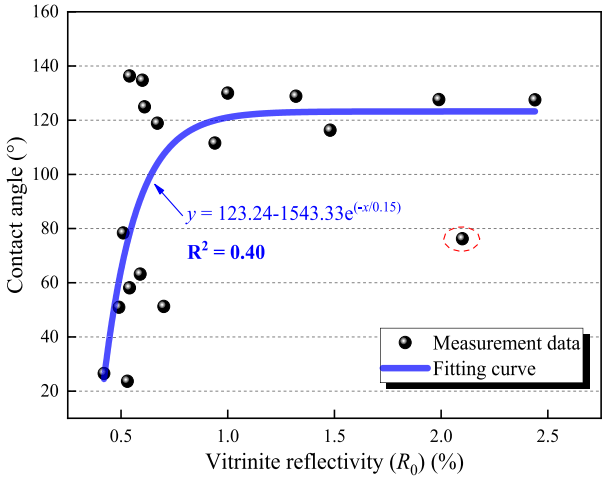

Figure 11. Variation of the contact angle between OCD and water with R_0.

individual protection, dust collector and spray dust removal devices in underground coal mines. That is, to reduce the coal dust concentration in coal mining sites, the particle size of spray mist should be 20−30 μm, and the filter particle size of dry dust collector should be less than 30 μm. Furtherly, because the smaller the particle size of coal dust, the greater the harm to the human body,[20] the government should fully consider the coal dust particle size parameter when specifying the maximum allowable dust concentration in underground coal mining face.

4.2. Pore Structure of the OCD. The pore structure of coal dust significantly influences its aerodynamic characteristics.[76] Specifically, the more developed the pore structure of coal dust, the larger its SSA and the lower its true density, thus the longer floating time in the air, leading to an increased probability of coal dust being inhaled by humans and consequently enhanced the harmfulness of coal dust to the human body.[38] In the same volume, coal dust with well-developed pores experiences less gravitational force and is more prone to diffusion in underground tunnels, making it easier to diffuse.[38] As shown in Figure 17b,c, although the two dust particles have the same particle size, the dust particles in Figure 17c have a more developed pore structure. This allowed the surface to adsorb more air, forming an air film and greater air buoyancy on the particle. Therefore, compared with the dust particles in Figure 17b, the particles in Figure 17c can disperse over a greater distance in underground tunnels. As shown in Figure 17d, the smaller dust particles experienced a relatively low gravitational force, allowing them to be easily lifted and carried by the air in underground tunnels. This enables them to disperse over a greater distance than larger dust particles. Therefore, the dust diffusion distance should be considered for dust control in the underground coal mining face, and the installation distance of spray and dust-collector should be increased, to improve the control efficiency of fine coal dust.

https://doi.org/10.1021/acsomega.4c06729
ACS Omega 2025, 10, 5379−5394

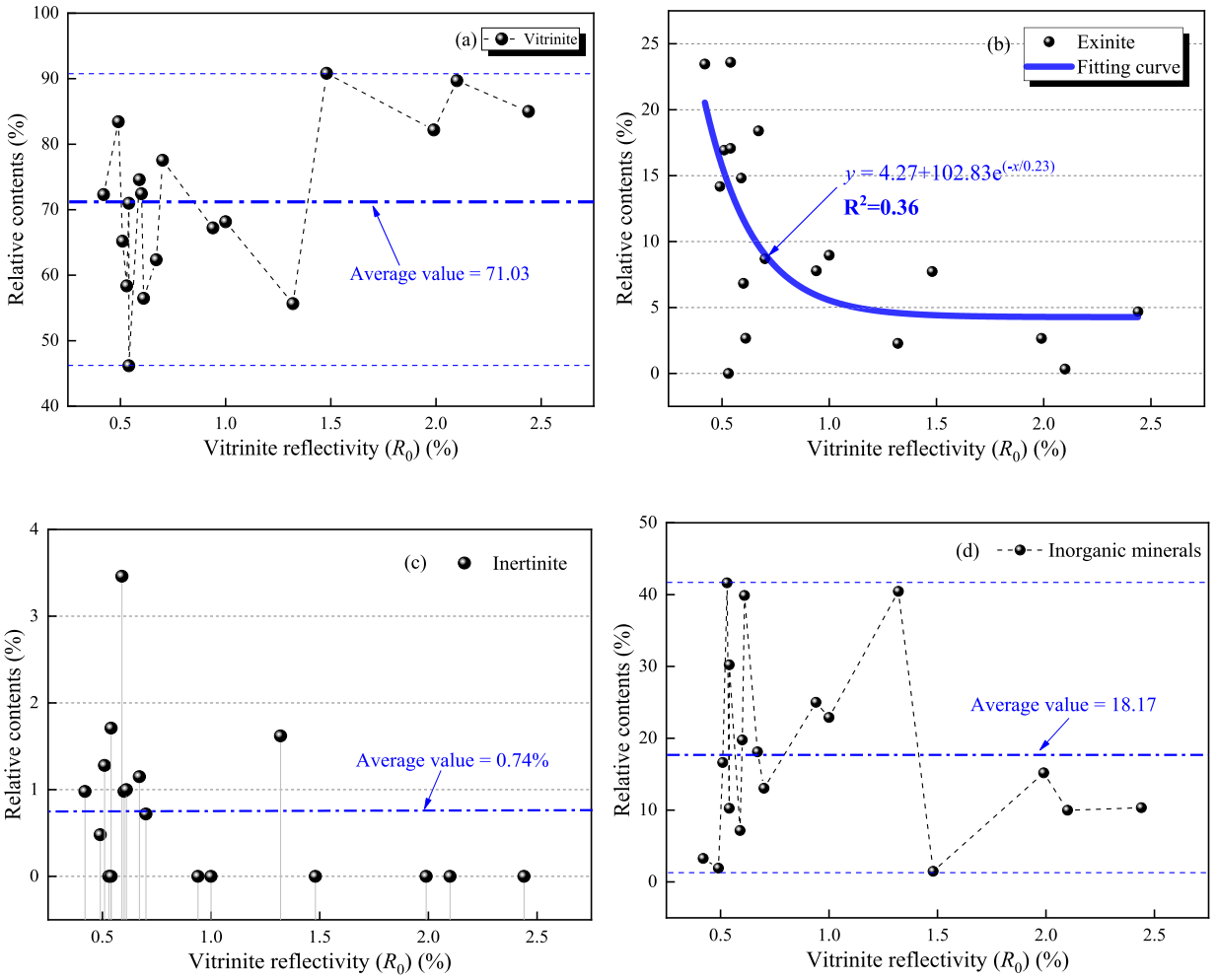

Figure 12. Variation of the vitrinite component of OCD with R_0: vitrinite (a), exinite (b), inertinite (c), and inorganic minerals (d).

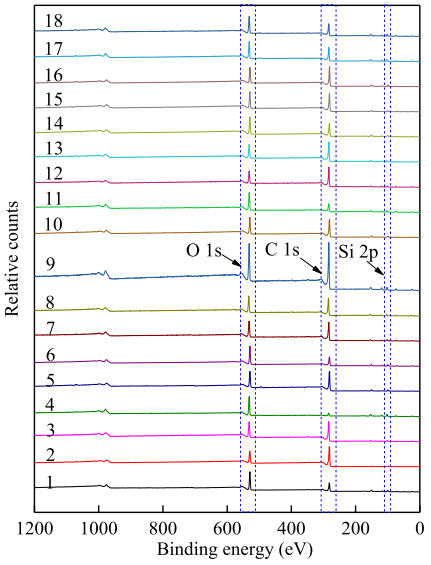

Figure 13. X-ray photoelectron spectrum (XPS) of OCD samples.

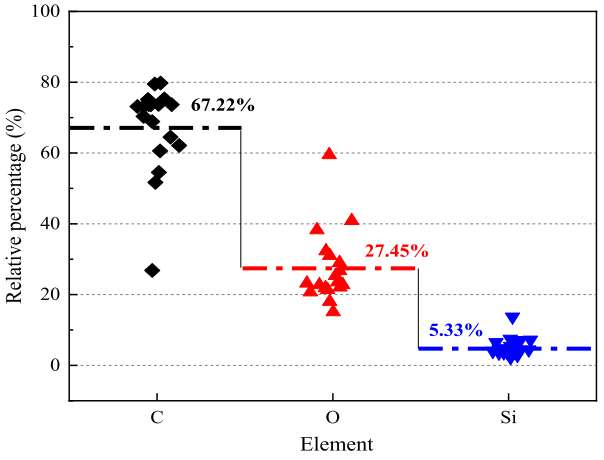

Figure 14. Relative content of the C, O, and Si elements on the OCD surface based on the XPS test.

4.3. Surface Oxidation Degree of the OCD. In addition, the large RCs of O, C, and the surface C−O functional groups in OCD, indicate that the degree of oxidation on the OCD surface is high, mainly due to the small particle size, large surface area, and well-developed pore structure of OCD, which allow the surface to adsorb a large amount of oxygen, resulting in a high degree of oxidation. Numerous studies[31,33−35] show that the oxygen-containing functional groups in coal dust can easily form hydrogen bonds with water molecules because of its strong polarity, thereby could increase the wettability of coal dust. Therefore, the greater the content of oxygen-containing functional groups in coal dust, the stronger the wettability of coal dust. In addition, studies[44,48] have shown that the oxygen-

https://doi.org/10.1021/acsomega.4c06729
ACS Omega 2025, 10, 5379−5394

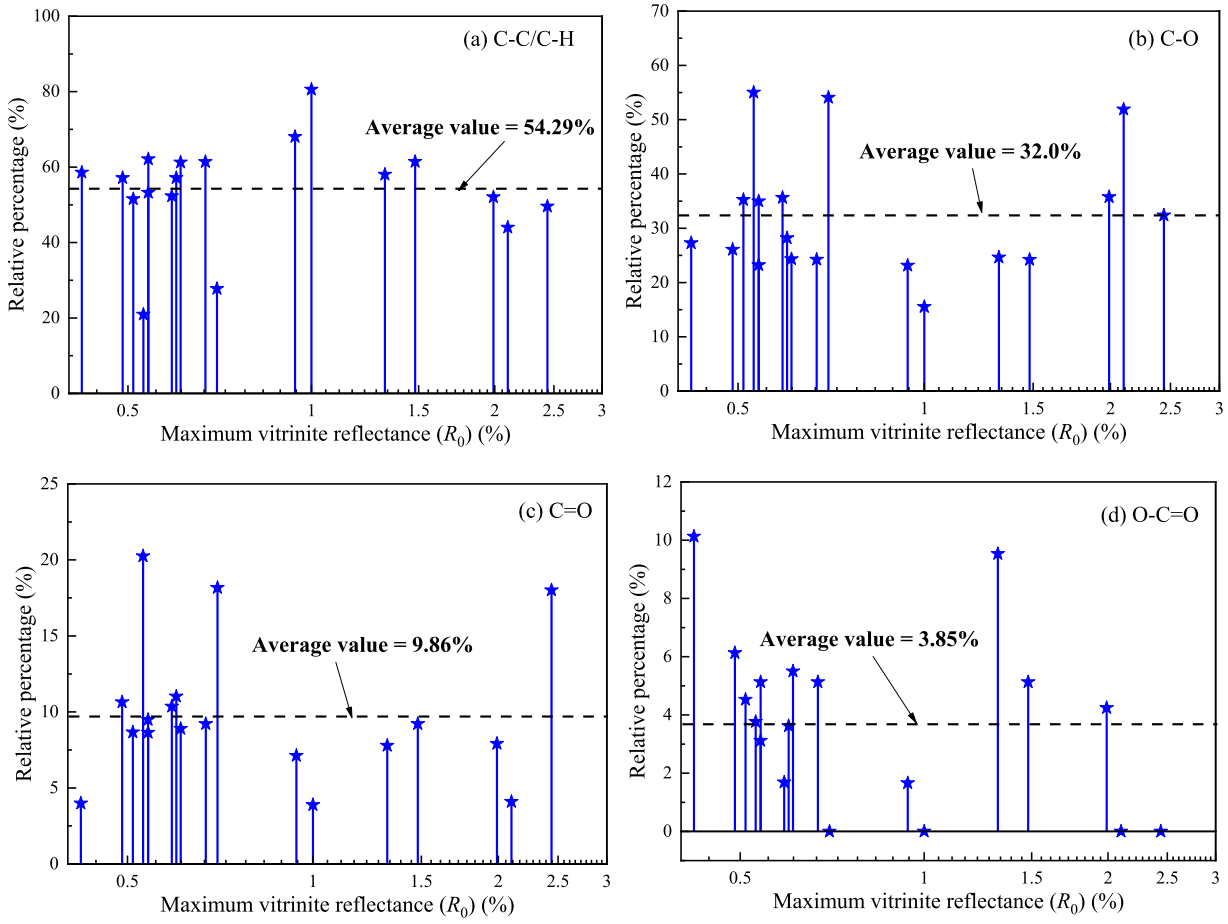

Figure 15. Variation of the functional carbon groups relative content on the surface of OCD with R_0: C−C and C−H (a), C−O (b), C═O (c), and O−C═O (d).

Table 4. Physicochemical Parameters of the OCD

number	physicochemical characterization	factors	number	physicochemical characterization	factors
1	wettability	contact angle	17		C
2		D10	18		H
3	particle size	D50	19	ultimate analysis	O
4		D90	20		N
5		P10	21		S
6		specific surface area (SSA)	22		C−C/C-H
7		mesopore size	23		C−O
8	pore properties	micropore size	24	surface functional groups	C═O
9		average pore size	25		O−C═O
10		mesopore volume	26		C
11		micropore volume	27		O
12		total pore volume	28		Si
13		moisture	29		vitrinite
14	industrial component	volatile	30	vitrinite component	exinite
15		ash	31		inertinite
16		fixed carbon	32		inorganic minerals

containing functional groups in coal dust also have a significant impact on its explosion and toxicity. Therefore, specific research on the explosion and toxicity of OCD should be carried out in the future.

4.4. Correlation Between the Physicochemical Parameters of the OCD and R_0. Furthermore, significant correlations between the physicochemical parameters of the OCD and R_0 were found in this study, which attributed to the fact that coal dust originates from coal seams. Specifically, as the coalification degree increases, the C content increases, the O content decreases, the porosity and the moisture content of coal all decreases, resulting in poorer wettability of coal dust. Therefore, for the coal with a high degree of coalification, dry dust removal technology should be preferentially selected during controlling coal dust. When applying wet dust removal technology, surfactant materials should be added to reduce the

https://doi.org/10.1021/acsomega.4c06729
ACS Omega 2025, 10, 5379−5394

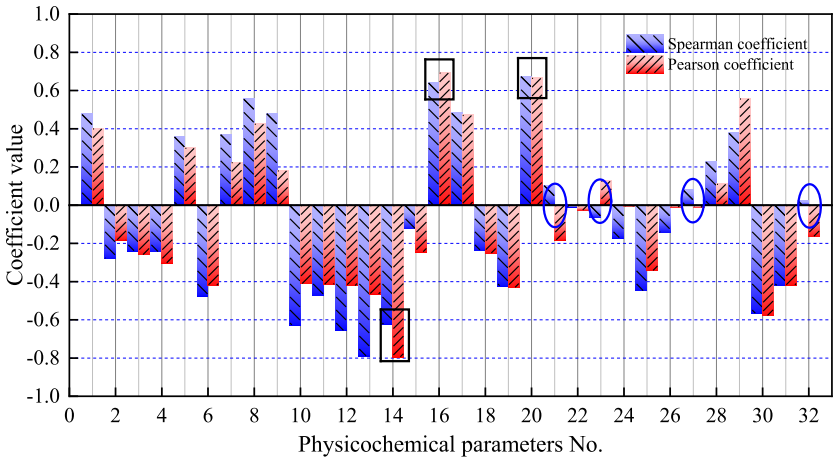

Figure 16. Spearman and Pearson coefficient between the physicochemical parameters of the original coal dust and the maximum vitrinite reflectance (R_0).

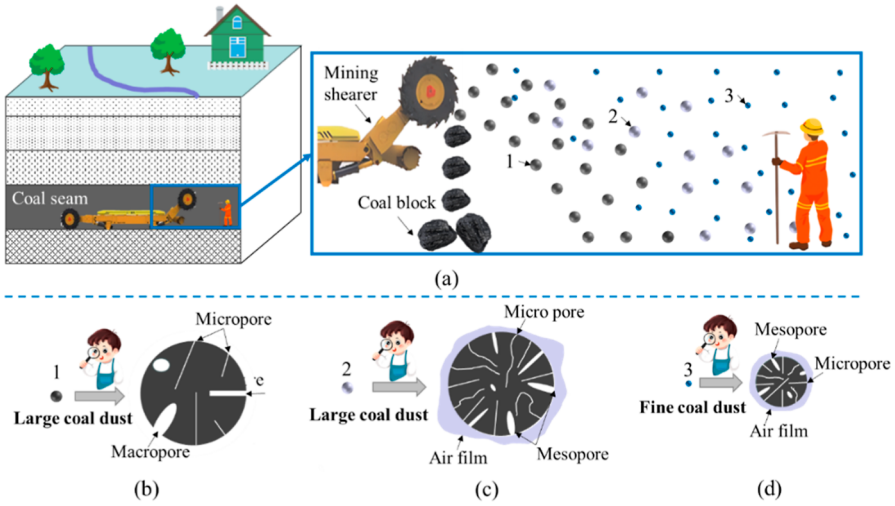

Figure 17. Diffusion of coal dust in underground mining sites (a) and the schematic diagrams of the large coal dust with undeveloped pore structure (b), large coal dust with developed pore structure (c), and fine coal dust with developed pore structure (d).

surface tension of water and improve the wettability of coal dust.

This study has some limitations, though we systematically collected and characterized the OCD and its physicochemical properties at various underground mining sites. First, when characterizing the physicochemical properties of coal dust, multiple methods can be used to improve the accuracy of test results; for instance, both scanning electron microscope (SEM) and laser particle size analyzer can be simultaneously employed to measure the particle size distribution of coal dust. Also, the method and device of sampling large amounts of original coal dust from underground air are very important, which should be carried out in the future.

To sum up, first time, we collected 18 OCD samples from underground coal mines for the first time. By characterizing the physicochemical parameters of OCD samples, it was found that compared to lab-crushed coal dust, the OCD exhibits significant characteristics such as smaller particle size, well-developed pore structure, and higher degree of oxidation. This provides a foundation for accurately understanding the harm of underground coal dust to human health and improving the efficiency of dust suppression technologies.

5. CONCLUSIONS

In this study, 18 OCD samples were collected from underground coal mining sites, and their physicochemical parameters were measured. The relationship between the physicochemical parameters of OCD and R_0 was investigated. The main conclusions are as follows:

1 OCD particles have small particle sizes. The average particle size (D50) of OCD was 26.49 μm, and 21% of OCD samples had a particle size <10 μm (P10). This particle size is significantly smaller than that of the lab-crushed coal dust.

2 OCD samples exhibited a well-developed pore structure. On average, the total pore volume of OCD is 8.24 × 10^{-3} cm^3/g, and the SSA of OCD is 8.24 m^2/g. With increasing R_0, the pore size of OCD varied as a cubic function, and the pore volume and SSA of the OCD decreased exponentially.

3 OCD exhibited a high degree of oxidation. With an increase in R_0, the O content in OCD decreased slightly, with an average of 32.35%, and the total average relative content of the O-containing functional groups in OCD, including C−O, C═O, and O−C═O, reached 45.71%.

https://doi.org/10.1021/acsomega.4c06729
ACS Omega 2025, 10, 5379−5394

This is mainly due to the small particle size and well-developed pore structure of OCD.

4 Among the 32 physicochemical parameters of OCD, 10 and 6 parameters had moderate and high correlations with R_0, respectively, which mainly represented wettability, pore structure, moisture content, and element content.

AUTHOR INFORMATION

Corresponding Author

Jianguo Liu − *NHC Key Laboratory for Engineering Control of Dust Hazard, University of Science and Technology Beijing, Beijing 100083, China; State Key Laboratory of Safety and Health for Metal Mine, Maanshan 243000, China; Research Institute of Macro-Safety Science, University of Science and Technology Beijing, Beijing 100083, China;* orcid.org/0000-0003-0736-6550; Phone: 86-18811343229; Email: liujg@ustb.edu.cn

Authors

Yuzhu Zhou − *NHC Key Laboratory for Engineering Control of Dust Hazard, University of Science and Technology Beijing, Beijing 100083, China; Research Institute of Macro-Safety Science, University of Science and Technology Beijing, Beijing 100083, China*

Longzhe Jin − *NHC Key Laboratory for Engineering Control of Dust Hazard, University of Science and Technology Beijing, Beijing 100083, China; Research Institute of Macro-Safety Science, University of Science and Technology Beijing, Beijing 100083, China*

Gang Li − *State Key Laboratory of Safety and Health for Metal Mine, Maanshan 243000, China*

Gang Zhou − *College of Safety and Environmental Engineering, Shandong University of Science and Technology, Qingdao 266590, China;* orcid.org/0000-0003-2440-8417

Minglei Lin − *NHC Key Laboratory for Engineering Control of Dust Hazard, University of Science and Technology Beijing, Beijing 100083, China; Research Institute of Macro-Safety Science, University of Science and Technology Beijing, Beijing 100083, China*

Shengnan Ou − *NHC Key Laboratory for Engineering Control of Dust Hazard, University of Science and Technology Beijing, Beijing 100083, China; Research Institute of Macro-Safety Science, University of Science and Technology Beijing, Beijing 100083, China*

Linquan Tong − *National Center for Occupational Safety and Health, National Health Commission of the People's Republic of China, Beijing 102308, China*

Weijun Zhang − *National Center for Occupational Safety and Health, National Health Commission of the People's Republic of China, Beijing 102308, China*

Xiaobing Wang − *NHC Key Laboratory for Engineering Control of Dust Hazard, University of Science and Technology Beijing, Beijing 100083, China*

Hong Gao − *NHC Key Laboratory for Engineering Control of Dust Hazard, University of Science and Technology Beijing, Beijing 100083, China; Research Institute of Macro-Safety Science, University of Science and Technology Beijing, Beijing 100083, China*

Complete contact information is available at: https://pubs.acs.org/10.1021/acsomega.4c06729

Notes

The authors declare no competing financial interest.

Consent to participate: All authors consent to participate the manuscript.

Consent for publication: All authors consent to publish the manuscript.

ACKNOWLEDGMENTS

This work was financially supported by the National Nature Science Foundation of China (nos 52204198, 52474205), the National Key Research and Development Program of China (no. 2022YFC2903901), the State Key Laboratory of Safety and Health for Metal Mines (2022-JSKSSYS-02), and the Fundamental Research Funds for the Central Universities (no. FRF-TP-22-115A1).

REFERENCES

(1) Gopinathan, P.; Santosh, M. S.; Kumar, O. P.; Subramani, T.; Antoniadis, V.; Shaheen, S. M.; Santosh, M. Mineralogical and geochemical characterization of coal debris from major coal fields in India: Implications on respirable dust hazards. *Process Saf. Environ. Prot.* **2024**, *184*, 1057−1068.

(2) Kamanzi, C.; Becker, M.; Jacobs, M.; Konečný, P.; Von Holdt, J.; Broadhurst, J. The impact of coal mine dust characteristics on pathways to respiratory harm: investigating the pneumoconiotic potency of coals. *Environ. Geochem. Health* **2023**, *45* (10), 7363−7388.

(3) Zhang, J.; Gu, H.; Chen, S.; Ai, W.; Dang, Y.; Ai, S.; Li, Z. Assessment of heavy metal pollution and preschool children health risk in urban street dusts from different functional areas in a typical industrial and mining city, NW China. *Environ. Geochem. Health* **2023**, *45* (10), 7199−7214.

(4) Kumari, M.; Kumar, A.; Bhattacharya, T. Assessment of heavy metal contamination in street dust: concentrations, bioaccessibility, and human health risks in coal mine and thermal power plant complex. *Environ. Geochem. Health* **2023**, *45* (10), 7339−7362.

(5) Miranda-Guevara, A.; Muñoz-Acevedo, A.; Fiorillo-Moreno, O.; Acosta-Hoyos, A.; Pacheco-Londoño, L.; Quintana-Sosa, M.; De Moya, Y.; Dias, J.; de Souza, G. S.; Martinez-Lopez, W.; et al. The dangerous link between coal dust exposure and DNA damage: unraveling the role of some of the chemical agents and oxidative stress. *Environ. Geochem. Health* **2023**, *45* (10), 7081−7097.

(6) Castranova, V.; Vallyathan, V. Silicosis and coal workers' pneumoconiosis. *Environ. Health Perspect.* **2000**, *108* (suppl 4), 675−684.

(7) Wang, B.; Wu, C.; Kang, L.; Reniers, G.; Huang, L. Work safety in China's Thirteenth Five-Year plan period (2016−2020): Current status, new challenges and future tasks. *Saf. Sci.* **2018**, *104*, 164−178.

(8) Bao, Q.; Nie, W.; Liu, C.; Zhang, H.; Wang, H.; Jin, H.; Yan, J.; Liu, Q. The preparation of a novel hydrogel based on crosslinked polymers for suppressing coal dusts. *J. Cleaner Prod.* **2020**, *249*, 119343.

(9) Hendryx, M.; Islam, M. S.; Dong, G. H.; Paul, G. Air pollution emissions 2008−2018 from Australian coal mining: Implications for public and occupational health. *Int. J. Environ. Res. Public Health* **2020**, *17* (5), 1570.

(10) Doney, B. C.; Blackley, D.; Hale, J. M.; Halldin, C.; Kurth, L.; Syamlal, G.; Laney, A. S. Respirable coal mine dust in underground mines, United States, 1982−2017. *Am. J. Ind. Med.* **2019**, *62* (6), 478−485.

(11) Glass, D. C.; Cohen, R.; Roberts, M.; Almberg, K.; Hoy, R.; Go, L.; Sim, M. R. 1497 Review of the respiratory component of the queensland coal mine workers' health scheme. *Occup. Environ. Med.* **2018**, *75* (Suppl2), A438.

(12) Zhang, J.; Xu, K.; Reniers, G.; You, G. Statistical analysis the characteristics of extraordinarily severe coal mine accidents

(ESCMAs) in China from 1950 to 2018. *Process Saf. Environ. Prot.* **2020**, *133*, 332−340.
(13) Qian, J.; Liu, Z.; Lin, S.; Li, X.; Ali, M. Study on microstructure characteristics of material evidence in coal dust explosion and its significance in accident investigation. *Fuel* **2020**, *265*, 116992.
(14) Zheng, Y. P.; Feng, C. G.; Jing, G. X.; Qian, X. M.; Li, X. J.; Liu, Z. Y.; Huang, P. A statistical analysis of coal mine accidents caused by coal dust explosions in China. *J. Loss Prev. Process Ind.* **2009**, *22* (4), 528−532.
(15) Gopinathan, P.; Subramani, T.; Barbosa, S.; Yuvaraj, D. Environmental impact and health risk assessment due to coal mining and utilization. *Environ. Geochem. Health* **2023**, *45* (10), 6915−6922.
(16) Yu, H. Mining waste: curb risks to people and the environment. *Nature* **2023**, *615* (7953), 586.
(17) Yu, H.; Zahidi, I.; Chow, M. F.; Liang, D.; Madsen, D. Ø. Reimagining Resources Policy: Synergizing Mining Waste Utilization for Sustainable Construction Practices. *J. Cleaner Prod.* **2024**, *464*, 142795.
(18) Song, S.; Peng, R.; Wang, Y.; Cheng, X.; Niu, R.; Ruan, H. Spatial distribution characteristics and risk assessment of soil heavy metal pollution around typical coal gangue hill located in Fengfeng Mining area. *Environ. Geochem. Health* **2023**, *45* (10), 7215−7236.
(19) Zhou, Q.; Qin, B. Coal dust suppression based on water mediums: A review of technologies and influencing factors. *Fuel* **2021**, *302*, 121196.
(20) Liu, T.; Liu, S. The impacts of coal dust on miners' health: a review. *Environ. Res.* **2020**, *190*, 109849.
(21) Abbasi, B.; Wang, X.; Chow, J. C.; Watson, J. G.; Peik, B.; Nasiri, V.; Riemenschnitter, K. B.; Elahifard, M. Review of respirable coal mine dust characterization for mass concentration, size distribution and chemical composition. *Minerals* **2021**, *11* (4), 426.
(22) Vanka, K. S.; Shukla, S.; Gomez, H. M.; James, C.; Palanisami, T.; Williams, K.; Horvat, J. C.; Britton, W. J.; Ilic, D.; Hansbro, P. M.; et al. Understanding the pathogenesis of occupational coal and silica dust-associated lung disease. *Eur. Respir. J.* **2022**, *31* (165), 210250.
(23) Beer, C.; Kolstad, H. A.; Søndergaard, K.; Bendstrup, E.; Heederik, D.; Olsen, K. E.; Omland, Ø.; Petsonk, E.; Sigsgaard, T.; Sherson, D. L.; et al. A systematic review of occupational exposure to coal dust and the risk of interstitial lung diseases. *Eur. Clin. Respir. J.* **2017**, *4* (1), 1264711.
(24) Beeckmans, J. M. The deposition of aerosols in the respiratory tract: I. Mathematical analysis and comparison with experimental data. *Can. J. Physiol. Pharmacol.* **1965**, *43* (1), 157−172.
(25) Marsalek, R.; Sassikova, M. Characterization of the size distribution of subbituminous coal by laser diffraction. *Instrum. Sci. Technol.* **2016**, *44* (3), 233−240.
(26) Mischler, S. E.; Cauda, E. G.; Di Giuseppe, M.; McWilliams, L. J.; Croix, C.; Sun, M.; Franks, J.; Ortiz, L. A. Differential activation of RAW 264.7 macrophages by size-segregated crystalline silica. *J. Occup. Med. Toxicol.* **2016**, *11*, 57.
(27) Wang, T.; Liu, J.; Wang, S.; Jin, L.; Lin, M.; Ou, S. Enhancement of the wettability of a coal seam during water injection: effect and mechanism of surfactant concentrations above the CMC. *Environ. Sci. Pollut. Res.* **2023**, *30* (14), 39857−39870.
(28) Zhou, Q.; Qin, B.; Li, H.; Hou, J. Changes of physical properties of coal dust with crush degrees and their effects on dust control ability of the surfactant solution spray. *Environ. Sci. Pollut. Res.* **2022**, *29*, 33785−33795.
(29) Zhang, H.; Nie, W.; Yan, J.; Bao, Q.; Wang, H.; Jin, H.; Peng, H.; Chen, D.; Liu, Z.; Liu, Q. Preparation and performance study of a novel polymeric spraying dust suppression agent with enhanced wetting and coagulation properties for coal mine. *Powder Technol.* **2020**, *364*, 901−914.
(30) Wang, P.; Han, H.; Tian, C.; Liu, R.; Jiang, Y. Experimental study on dust reduction via spraying using surfactant solution. *Atmos. Pollut. Res.* **2020**, *11* (6), 32−42.
(31) Wang, P.; Han, H.; Liu, R.; Li, Y.; Tan, X. Effects of metamorphic degree of coal on coal dust wettability and dust-suppression efficiency via spraying. *Adv. Mater. Sci. Eng.* **2020**, *2020* (1), 4854391.
(32) Liu, J. G.; Jin, L. Z.; Wang, J. Y.; Ou, S. N.; Wang, T. Y. Co-influencing mechanisms of physicochemical properties of blasting dust in iron mines on its wettability. *Int. J. Miner., Metall. Mater.* **2019**, *26*, 1080−1091.
(33) Zhou, Q.; Qin, B.; Wang, J.; Wang, H.; Wang, F. Experimental investigation on the changes of the wettability and surface characteristics of coal dust with different fractal dimensions. *Colloids Surf., A* **2018**, *551*, 148−157.
(34) Shi, Q.; Qin, B.; Bi, Q.; Qu, B. Changes in the surface structure of coal caused by igneous intrusions and their effect on the wettability. *Energy Fuels* **2018**, *32* (9), 9371−9379.
(35) Xu, C.; Wang, D.; Wang, H.; Xin, H.; Ma, L.; Zhu, X.; Zhang, Y.; Wang, Q. Effects of chemical properties of coal dust on its wettability. *Powder Technol.* **2017**, *318*, 33−39.
(36) Ma, Q.; Nie, W.; Yang, S.; Xu, C.; Peng, H.; Liu, Z.; Guo, C.; Cai, X. Effect of spraying on coal dust diffusion in a coal mine based on a numerical simulation. *Environ. Pollut.* **2020**, *264*, 114717.
(37) Ali, M.; Yan, C.; Sun, Z.; Wang, J.; Gu, H. CFD simulation of dust particle removal efficiency of a venturi scrubber in CFX. *Nucl. Eng. Des.* **2013**, *256*, 169−177.
(38) Liu, J.; Wang, S.; Jin, L.; Wei, Y.; Ou, S.; Wang, T.; Xu, J.; Liu, X.; Tao, G. Surface pore characteristics of original coal dust produced in underground mining sites and their impact on the moisture content. *Process Saf. Environ. Prot.* **2022**, *167*, 284−298.
(39) Yu, H.; Zahidi, I.; Liang, D. Sustainable porous-insulation concrete (SPIC) material: recycling aggregates from mine solid waste, white waste and construction waste. *J. Mater. Res. Technol.* **2023**, *23*, 5733−5745.
(40) Yang, J.; Wu, X.; Gao, J.; Li, G. Surface characteristics and wetting mechanism of respirable coal dust. *Min. Sci. Technol.* **2010**, *20* (3), 365−371.
(41) Xue, X. Prediction for the burnout of pulverized coal in a coal-fired power plant by combining proximate analysis, coal petrography, and pulverized-coal size distribution. *Energy Sources, Part A* **2016**, *38* (1), 69−74.
(42) Samanli, S.; Cuhadaroglu, D.; Hwang, J. Y. An investigation of particle size variation in stirred mills in terms of breakage kinetics. *Energy Sources, Part A* **2011**, *33* (6), 549−561.
(43) Zhou, W.; Wang, H.; Wang, D.; Du, Y.; Zhang, K.; Qiao, Y. An experimental investigation on the influence of coal brittleness on dust generation. *Powder Technol.* **2020**, *364*, 457−466.
(44) Trechera, P.; Moreno, T.; Córdoba, P.; Moreno, N.; Zhuang, X.; Li, B.; Li, J.; Shangguan, Y.; Kandler, K.; Dominguez, A. O.; et al. Mineralogy, geochemistry and toxicity of size-segregated respirable deposited dust in underground coal mines. *J. Hazard. Mater.* **2020**, *399*, 122935.
(45) Kollipara, V. K.; Chugh, Y. P.; Mondal, K. Physical, mineralogical and wetting characteristics of dusts from Interior Basin coal mines. *Int. J. Coal Geol.* **2014**, *127*, 75−87.
(46) Yang, T.; Han, Y. P.; Li, L.; Liu, J. X. Microbial Properties of Different Size Aerosols at Human Average Respiratory Height During Fog-haze Days. *Huanjing Kexue* **2019**, *40* (4), 1680−1687.
(47) Xu, G.; Chen, Y.; Eksteen, J.; Xu, J. Surfactant-aided coal dust suppression: A review of evaluation methods and influencing factors. *Sci. Total Environ.* **2018**, *639*, 1060−1076.
(48) Zhang, J.; Xu, P.; Sun, L.; Zhang, W.; Jin, J. Factors influencing and a statistical method for describing dust explosion parameters: a review. *J. Loss Prev. Process Ind.* **2018**, *56*, 386−401.
(49) Liu, G.; Xu, Q.; Zhao, J.; Nie, W.; Guo, Q.; Ma, G. Research status of pathogenesis of pneumoconiosis and dust control technology in mine—a review. *Appl. Sci.* **2021**, *11* (21), 10313.
(50) Wang, H.; Zhang, L.; Wang, D.; He, X. Experimental investigation on the wettability of respirable coal dust based on infrared spectroscopy and contact angle analysis. *Adv. Powder Technol.* **2017**, *28* (12), 3130−3139.

https://doi.org/10.1021/acsomega.4c06729
ACS Omega 2025, 10, 5379−5394

(51) Nie, B.; Liu, X.; Yang, L.; Meng, J.; Li, X. Pore structure characterization of different rank coals using gas adsorption and scanning electron microscopy. *Fuel* **2015**, *158*, 908−917.
(52) Brunauer, S.; Emmett, P. H.; Teller, E. Adsorption of gases in multimolecular layers. *J. Am. Chem. Soc.* **1938**, *60* (2), 309−319.
(53) Horváth, G.; Kawazoe, K. Method for the calculation of effective pore size distribution in molecular sieve carbon. *J. Chem. Eng. Jpn.* **1983**, *16* (6), 470−475.
(54) Barrett, E. P.; Joyner, L. G.; Halenda, P. P. The determination of pore volume and area distributions in porous substances. I. Computations from nitrogen isotherms. *J. Am. Chem. Soc.* **1951**, *73* (1), 373−380.
(55) Seaton, N. A.; Walton, J. P. R. B.; quirke, N. A new analysis method for the determination of the pore size distribution of porous carbons from nitrogen adsorption measurements. *Carbon* **1989**, *27* (6), 853−861.
(56) Zazouli, M. A.; Dehbandi, R.; Mohammadyan, M.; Aarabi, M.; Dominguez, A. O.; Kelly, F. J.; Khodabakhshloo, N.; Rahman, M. M.; Naidu, R. Physico-chemical properties and reactive oxygen species generation by respirable coal dust: Implication for human health risk assessment. *J. Hazard. Mater.* **2021**, *405*, 124185.
(57) Liu, J.; Wang, S.; Jin, L.; Wang, T.; Zhou, Z.; Xu, J. Water-retaining properties of NCZ composite dust suppressant and its wetting ability to hydrophobic coal dust. *Int. J. Coal Sci. Technol.* **2021**, *8*, 240−247.
(58) Jin, L.; Liu, J.; Guo, J.; Wang, J.; Wang, T. Physicochemical factors affecting the wettability of copper mine blasting dust. *Int. J. Coal Sci. Technol.* **2021**, *8*, 265−273.
(59) Liu, X.; Song, D.; He, X.; Nie, B.; Wang, Q.; Sun, R.; Sun, D. Coal macromolecular structural characteristic and its influence on coalbed methane adsorption. *Fuel* **2018**, *222*, 687−694.
(60) Zhou, G.; Xu, C.; Cheng, W.; Zhang, Q.; Nie, W. Effects of oxygen element and oxygen-containing functional groups on surface wettability of coal dust with various metamorphic degrees based on XPS experiment. *J. Anal. Methods Chem.* **2015**, *2015* (1), 1−8.
(61) Wang, J.; He, Y.; Zhang, Y.; Zhao, X.; Peng, Z.; Wang, S.; Zhang, T. Research on cationic surfactant adsorption performance on different density lignite particles by XPS nitrogen analysis. *Fuel* **2018**, *213*, 48−54.
(62) Woche, S. K.; Goebel, M. O.; Mikutta, R.; Schurig, C.; Kaestner, M.; Guggenberger, G.; Bachmann, J. Soil wettability can be explained by the chemical composition of particle interfaces-An XPS study. *Sci. Rep.* **2017**, *7* (1), 42877.
(63) Xia, W.; Yang, J.; Liang, C. Investigation of changes in surface properties of bituminous coal during natural weathering processes by XPS and SEM. *Appl. Surf. Sci.* **2014**, *293*, 293−298.
(64) Zhao, Z.; Chang, P.; Xu, G.; Ghosh, A.; Li, D.; Huang, J. Comparison of the coal dust suppression performance of surfactants using static test and dynamic test. *J. Cleaner Prod.* **2021**, *328*, 129633.
(65) Ding, X.; Wang, D.; Luo, Z.; Xu, G.; Wang, T.; Cheng, F. Investigation of agglomerating and wetting behaviour during coal dust suppression via the synergistic application of hydrocarbon and short-chain-fluorocarbon surfactants in the presence of electrolytes. *Powder Technol.* **2022**, *404*, 117518.
(66) Nie, W.; Tian, Q.; Niu, W.; Li, R.; Bao, Q.; Zhang, X.; Yan, X.; Lian, J. Synergistic effect of binary mixture of anionic nonionic surfactant on inhibiting coal dust pollution: Experiment and simulation. *J. Environ. Chem. Eng.* **2023**, *11* (3), 110099.
(67) Trechera, P.; Querol, X.; Lah, R.; Johnson, D.; Wrana, A.; Williamson, B.; Moreno, T. Chemistry and particle size distribution of respirable coal dust in underground mines in Central Eastern Europe. *Int. J. Coal Sci. Technol.* **2022**, *9* (1), 3.
(68) Cheng, J.; Zheng, X.; Lei, Y.; Luo, W.; Wang, Y.; Borowski, M.; Li, X.; Song, W.; Wang, Z.; Wang, K. A compound binder of coal dust wetting and suppression for coal pile. *Process Saf. Environ. Prot.* **2021**, *147*, 92−102.
(69) Zhou, G.; Fan, T.; Ma, Y. Preparation and chemical characterization of an environmentally-friendly coal dust cementing agent. *J. Chem. Technol. Biotechnol.* **2017**, *92* (10), 2699−2708.
(70) Zhang, Q.; Zhou, G.; Hu, Y.; Wang, W. Experimental investigation on wetting mechanism for coal dust with different metamorphic degree based on infrared spectrum and 13C-NMR. *Surf. Interface Anal.* **2020**, *52* (8), 470−485.
(71) Wang, X.; Yuan, S.; Jiang, B. Experimental investigation of the wetting ability of surfactants to coals dust based on physical chemistry characteristics of the different coal samples. *Adv. Powder Technol.* **2019**, *30* (8), 1696−1708.
(72) He, X.; Liu, X.; Nie, B.; Song, D. FTIR and Raman spectroscopy characterization of functional groups in various rank coals. *Fuel* **2017**, *206*, 555−563.
(73) Laxminarayana, C.; Crosdale, P. J. Role of coal type and rank on methane sorption characteristics of Bowen Basin, Australia coals. *Int. J. Coal Geol.* **1999**, *40* (4), 309−325.
(74) Xu, C.; Zhou, G.; Qiu, H. Analysis of the microscopic mechanism of coal wettability evolution in different metamorphic states based on NMR and XPS experiments. *RSC Adv.* **2017**, *7* (76), 47954−47965.
(75) Liu, X.; Song, D.; He, X.; Nie, B.; Wang, L. Insight into the macromolecular structural differences between hard coal and deformed soft coal. *Fuel* **2019**, *245*, 188−197.
(76) Kong, W.; Dong, H.; Wu, J.; Zhao, Y.; Jin, Z. Experimental study on the effect of porous media on the aerodynamic performance of airfoils. *Aerospace* **2023**, *10* (1), 25.

https://doi.org/10.1021/acsomega.4c06729
ACS Omega 2025, 10, 5379−5394